Available online at www.sciencedirect.com
ScienceDirect
Bioorganic & Medicinal Chemistry Letters 18 (2008) 634–639
Bioorganic & Medicinal Chemistry Letters

Identification of 2-amino-5-(thioaryl)thiazoles as inhibitors of nerve growth factor receptor TrkA

Soong-Hoon Kim,[a,*] John S. Tokarski,[b] Kenneth J. Leavitt,[a] Brian E. Fink,[a] Mark E. Salvati,[a] Robert Moquin,[a] Mary T. Obermeier,[d] George L. Trainor,[a] Gregory G. Vite,[a] Linda K. Stadnick,[c] Jonathan S. Lippy,[c] Dan You,[c] Matthew V. Lorenzi[c] and Ping Chen[a]

[a]*Department of Oncology Chemistry, Bristol-Myers Squibb Research and Development, PO Box 4000, Princeton, NJ 08543-4000, USA*
[b]*Computer Aided Drug Design, Bristol-Myers Squibb Research and Development, PO Box 4000, Princeton, NJ 08543-4000, USA*
[c]*Discovery Biology, Bristol-Myers Squibb Research and Development, PO Box 4000, Princeton, NJ 08543-4000, USA*
[d]*Pharmaceutical Candidate Optimization, Bristol-Myers Squibb Research and Development, PO Box 4000, Princeton, NJ 08543-4000, USA*

Received 3 October 2007; revised 19 November 2007; accepted 19 November 2007
Available online 28 November 2007

Abstract—2-Amino-5-(thioaryl)thiazoles are potent inhibitors of TrkA (e.g., **20h**, TrkA IC_{50} = 0.6 nM) that show anti-proliferative effect in cellular assays. A proposed inhibitor binding mode to TrkA active site is consistent with key SAR observations.

TrkA (Troponyosin-receptor kinase A) is a cell surface receptor kinase containing an extracellular, a transmembrane, and a cytoplasmic kinase domain. The binding of a neurotrophin triggers oligomerization of the receptors, phosphorylation of tyrosine residues in the kinase domain, and activation of intercellular signaling pathways, including Ras/MAPK cascade, PI3K/AKT, and IP3-dependent Ca^{2+} release. The interaction of TrkA, along with related TrkB and C, with neurotrophins (NGF, BDNF, and NT-3) plays an important role for homeostasis of neural network, including differentiation, proliferation, and survival.[1–3] Several lines of evidence also suggest that the interplay of TrkA with NGF plays a critical role in the prognosis and outcome in several tumors.

For instance, an over-expression of TrkA correlates with an aggressive phenotype and poor clinical outcome in malignant melanomas,[4] ovarian carcinoma,[5] and pancreatic cancer.[6] In view of this, the on-going clinical trials of Trk inhibitors may provide valuable insights into anti-tumor efficacy and Trk inhibition.[7–9] In addition, other research groups have reported selective inhibitors of TrkA.[10,11] We report potent (TrkA IC_{50} < 0.001 μM) 2-amino-5-(thioaryl)thiazole inhibitors of TrkA, and provide evidence that their anti-proliferative effect against cell lines is due to selective inhibition of TrkA.

Screening of an in-house kinase deck with the criteria of (1) having activity against kinases at a pre-determined IC_{50} cut-off, and (2) maximizing structural diversity led to several potent hits. Among them, 2-amino-5-(thioaryl)thiazole **1** appeared especially promising due to its potent TrkA inhibition (TrkA IC_{50} = 0.05 μM, Fig. 1); and as a class, 2-amino-5-(aryl)thiazoles have

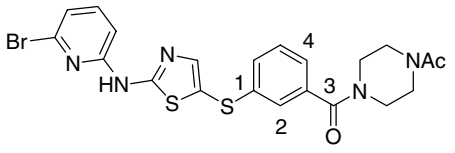

1: TrkA IC_{50} = 0.05 μM

Figure 1. Structure of initial TrkA screening hit.

Keywords: TrkA; Troponyosin-receptor kinase A; Nerve growth factor; NGF; Kinase inhibitor; 2-Amino-5-(thioaryl) thiazoles.
* Corresponding author. Tel.: +1 609 252 4079; fax: +1 609 252 3993; e-mail: soonghoon.kim@bms.com

0960-894X/$ - see front matter © 2007 Elsevier Ltd. All rights reserved.
doi:10.1016/j.bmcl.2007.11.076

shown favorable oral pK as selective inhibitors of Ikt (Interleukin-2-inducible T cell kinases).[12,13] The next set of TrkA inhibitors were designed toward establishing SAR around both pyridine and thioaryl rings; their syntheses are shown in Schemes 1–5.

The majority of compounds in Tables 1–4 follows a generalized synthetic route shown in Scheme 1, established previously for Ikt inhibitors.[12,13] Nitro ester **2** is reduced, converted to its transient diazo-compound with $NaNO_2$ and HCl, which is displaced with potassium ethylxanthate to afford xanthate **4**. Hydrolysis to thioacid **5**, followed by condensation with bromo-thiazole **9**[12] with NaOMe in methanol, gave the aminothiazole acid **10**. Both primary and secondary amides were prepared using BOP as the coupling reagent; yields ranged from 37% to 91% for a range of amides. For additional substituted pyridines (**6:** R^1 = H, Me, Br) and thioaryls (**4:** X = H, Me), the same synthetic route was employed (Scheme 1).

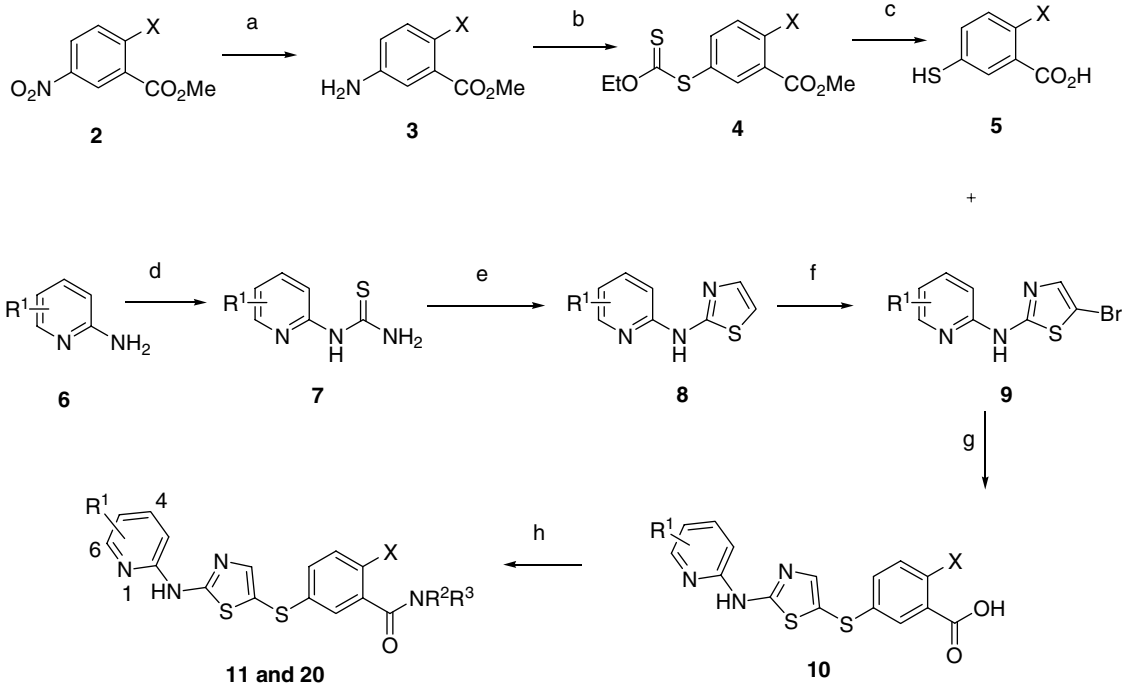

Scheme 1. For R^1 = H, X = Me (compounds **11h**, **11j**–**11t**, **19a**, **20a**, and **20c**). Reagents and conditions: (a) H_2 (balloon), 10% Pd (C), EtOAc, rt, 1.5 h, 96%; (b) $NaNO_2$, HCl, H_2O; $NaHCO_3$(s), KSCSOEt, H_2O, 45 °C, 1.5 h, 30%; (c) KOH, MeOH–H_2O, rt, 18 h, 78%; (d) SCNCOPh, acetone, 100%; aq NaOH, 73%; (e) $ClCH_2CHO$, aq ethanol, 79%; (f) Br_2, AcOH, 86%; (g) NaOMe, MeOH, 52 °C, 75%; (h) BOP, DIEA, DMF, rt (37–91%). Compounds **1**, **11a**–**b** (R^1 = 6-Br, X = H); **11c**, **11t**–**w**, **20d**, and **20g** (R^1 = 6-Br, X = methyl); **11d** (R^1 = H, X = H); **11f** (R^1 = 5-Br, X = H); and **11h** (R^1 = methyl, X = H) were prepared following the same general synthetic scheme.

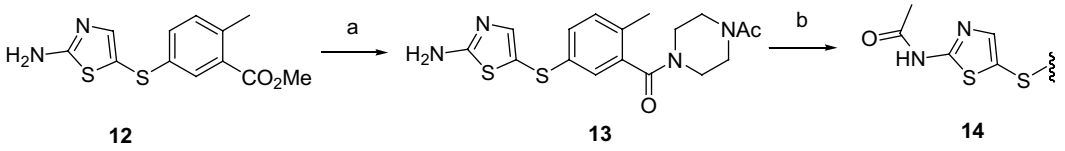

Scheme 2. Reagents: (a) KOH, MeOH/H_2O, 87%; *N*-acetylpiperazine, BOP, DIEA, DMF, 100%. (b) Ac_2O, DMAP, DCM, 25%.

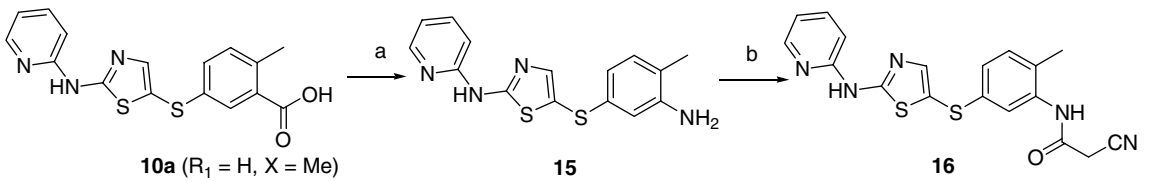

Scheme 3. Reagents and conditions: (a) DPPA, TEA, 1,4-dioxane, rt; $Me_3Si(CH_2)_2OH$, 75 °C; TFA, DCM, rt, 29% for three steps. (b) $NCCH_2CO_2H$, BOP, DIEA, DMF, rt, 13%.

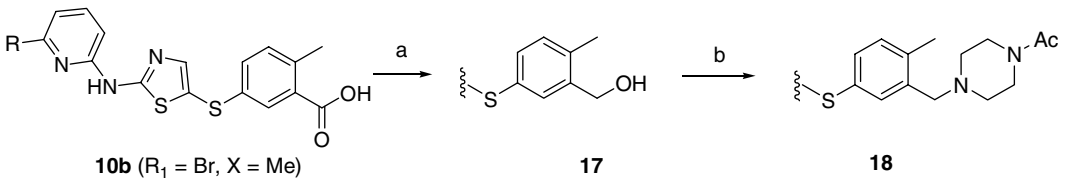

Scheme 4. Reagents and conditions: (a) CDI, THF, rt, 19 h; $NaBH_4$, H_2O, 76% for two steps. (b) MnO_2, DCE, 60 °C; *N*-acetyl piperazine, $NaCNBH_3$, ACN, 2%.

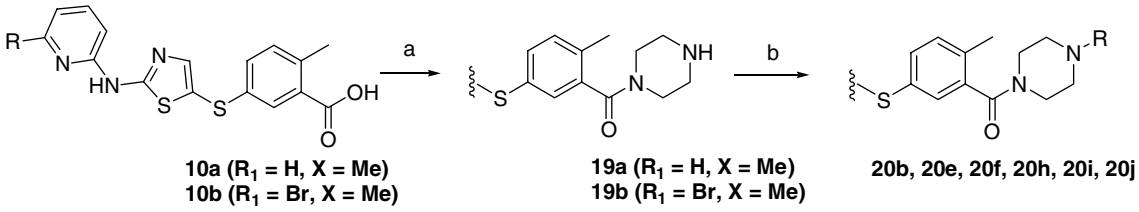

Scheme 5. Reagents and conditions: (a) Piperazine, BOP, DIEA, DMF, 51%. (b) BOP, DIEA, DMF, rt (**20b**: 49%; **20e**: 75%); **20h**: *N*-Boc glycine, BOP, DIEA, DMF, rt then TFA, DCM (41% for two steps); **20i**: *N*-Boc-L-alanine, BOP, DIEA, DMF, rt then TFA, DCM (65% for two steps); **20j**: *N*-Boc-D-alanine, BOP, DIEA, DMF, rt then TFA, DCM (67% for two steps); Compound **20f** was prepared from **20d** (BH_3-THF, 68 °C, 25%).

Table 1. SAR of terminal arylthio ring

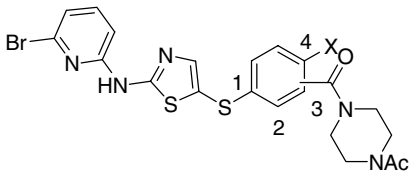

Compound	X	Regioisomer	Trk A IC_{50} (μM)[14]
1	H	1,3-Meta	0.050
11a	H	1,2-Ortho	1.9
11b	—	1,4-Para	1.3
11c	Me	1,3-Meta	0.001

Table 2. SAR of substituted pyridine ring

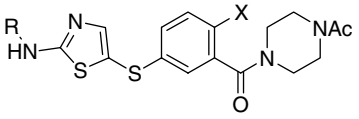

Compound	X	R	TrK A IC_{50} (μM)[14]
11d	H	2-Pyridyl	0.24
11e	H	2-(6-Bromo) Pyridyl	0.050
11f	H	2-(5-Bromo) Pyridyl	0.52
11g	H	2-(6-Methyl) Pyridyl	1.1
11h	Me	2-Pyridyl	0.080
11c	Me	2-(6-Bromo) Pyridyl	0.001
13	Me	H	>5.0
14	Me	Acetyl	>5.0

Several compounds were designed to address specific SAR questions. Synthesis of compounds **13** and **14**, which lack the pyridine ring, is shown in Scheme 2. Previously described ester **12**[13] is hydrolyzed and coupled to *N*-acetylpiperazine to give aminothiazole **13**, which is acylated with acetic anhydride to give compound **14**.

Table 3. SAR of acyclic amides

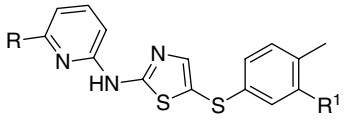

Compound	R	R^1	TrK A IC_{50} (μM)[14]
11j	H	$CONH_2$	0.79
11k	H	$CONHCH_2CH_3$	>5.0
11l	H	$CONHCHMe_2$	2.0
11m	H	$CONHCH_2CN$	0.044
11n	H	$CONHCH_2CCH$	1.2
11o	H	$CONHCH_2CH_2CN$	0.065
11p	H	$CONHCH_2CH_2OH$	0.76
11q	H	$CONHCH_2CH_2NHMe$	0.19
11r	H	$CONHCH_2CH_2NHAc$	0.32
11s	H	CONHBn	>5.00
11t	Br	$CON(Me)CH_2CN$	0.002
11u	Br	$CONHCH_2CH_2CN$	0.067
11v	Br	$CON(Me)\ CH_2CH_2CN$	0.010
11w	Br	$CON(Me)CH_2CH_2NHMe$	0.031
16	H	$NHCOCH_2CN$	0.060

Scheme 3 shows synthesis of a reverse amide of compound **11m**. Curtuis re-arrangement of compound **10a**, followed by TFA de-protection, gave aniline **15**. Cyanoacetic acid was coupled with compound **15** to give compound **16**. The synthesis of compound **18**, which lacks one amide carbonyl group from potent inhibitor **11c**, is shown in Scheme 4. The key step was the reductive amination with *N*-acetyl piperazine, following MnO_2 oxidation of alcohol **17**.

Synthesis of substituted piperazines (Table 5) is shown in Scheme 5, following standard acylation chemistry from compounds **19a** and **19b**.

As illustrated in Table 1, the 1,3-meta substitution (**1**: TrkA IC_{50} = 0.05 μM)[14] pattern in the thiophenyl ring is favored over others (**1** vs **11a**–**b**). In addition, a 50-fold

Table 4. SAR of substituted piperazines

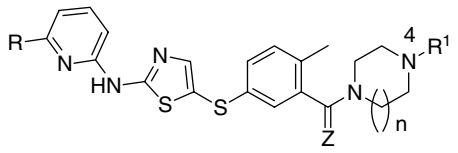

Compound	R	R^1	TrK A IC_{50} (μM)[14]
11h	H	COMe	0.080
18[a]	H	COMe	0.72
20a[b]	H	COMe	1.1
19a	H	H	0.16
20b	H	CO_2Me	0.21
20c	H	SO_2Me	0.91
20d	Br	COMe	0.001
20e	Br	COEt	0.021
20f	Br	CH_2Me	0.23
20g	Br	CH_2CONH_2	0.15
20h	Br	$COCH_2NH_2$	0.0006
20i	Br	COCHMe(S)NH2	0.001
20j	Br	COCHMe(R)NH2	0.001

[a] Z = H, H for compound **18**; all others are Z = Oxygen.
[b] *n* = 2 for compound **20a**; all others are *n* = 1.

Table 5. Antiproliferative effects of Trk A inhibitors[18]

Compound	Trk A IC_{50} (μM)	V3.1 IC_{50} (μM)	CD8-Trk A IC_{50} (μM)	SHSY5Y IC_{50} (μM)
20j	0.001	3.61	0.23	1.78
11c	0.001	2.28	0.25	1.14
11v	0.01	3.32	0.37	1.17
11t	0.002	3.0	0.39	0.75
11w	0.03	3.06	0.46	1.66
20h	0.0006	4.08	0.55	3.06
20i	0.001	3.52	1.15	4.26
11k	>5	>10	>10	>10

increase in potency is observed from X = H (**1**) and X = methyl (**11c**). This increase in potency by ortho-substitution appears general, as demonstrated by a 4-fold difference in potency between compound **11d** (X = H, TrkA IC_{50} = 0.24 μM, Table 2) and compound **11h** (X = Me, TrkA IC_{50} = 0.08 μM).

Next, the role of the pyridine ring in overall inhibition was explored (Table 2). Compound **13** that lacks the pyridine ring is essentially devoid of TrkA inhibition (IC_{50} > 5 μM) compared to control (**11h**: IC_{50} = 0.08 μM). Furthermore, the lack of activity of compound **14** (IC_{50} > 5 μM), with a basic carbonyl group, suggests that the pyridine provides more than a polar interaction through its basic nitrogen. This observation is further supported by the narrow SAR of the pyridine ring. Thus, a 5-fold increase from **11d** to **11e** (IC_{50} = 0.05 μM) is observed from a hydrogen to a bromine at C-6 position. The less polar methyl analog **11g** shows reduced TrkA inhibition (IC_{50} = 1.1 μM). Furthermore, the position of the bromine is critical. Compound **11f** (IC_{50} = 0.52 μM) with bromine at C-5 shows 10-fold decrease in activity relative to **11e**. Finally, the effect of changes on the thioaryl and pyridine rings appears additive. Compound **11c,** which has both an ortho-methyl group and a C-6 bromine group, shows potent inhibition (TrkA IC_{50} = 0.001 μM).

As shown in Table 3, acyclic amides (**11j–w**, **16**) are typically not as potent inhibitors of TrkA. Nevertheless, a subset of compounds show potent activity and consistent SAR, suggestive of a common pharmacophore. The 100-fold increase in potency from ethyl amide **11k** (IC_{50} > 5 μM) to isosteric nitrile **11m** (IC_{50} = 0.044 μM) is suggestive of a productive binding interaction of the nitrile group in the active site. This observation is further supported by the less active compound **11n** (IC_{50} = 1.2 μM), which contains a non-basic nitrile isostere. Compound **16**, a reverse amide isostere of **11m**, shows nearly identical activity (IC_{50} = 0.060 μM). Within a given series, an *N*-methylation appears to increase potency. Thus, there is a 7-fold increase from compound **11u** (IC_{50} = 0.067 μM) to compound **11v** (IC_{50} = 0.010 μM). *N*-methyl **11t** (IC_{50} = 0.002 μM) is a potent inhibitor of TrkA.

The role of substituted piperazine, a cyclic amide present in potent inhibitor **11c**, was explored and is summarized in Table 4. A 7-membered homopiperazine **20a** (IC_{50} = 0.72 μM) is less active than the piperazine **11h** (IC_{50} = 0.08 μM). A 9-fold loss in potency is observed when the amide carbonyl group next to the phenyl group is removed (**18**: IC_{50} = 0.72 μM), compared to control **11h**. The nature of distal N-4 carbonyl group also appears to play an important role in overall inhibition. Thus, compounds with a carbonate (**20b**: IC_{50} = 0.21 μM), or a sulfonamide (**20c**: IC_{50} = 0.91 μM), have lower potency than **11h**, even if both possess a basic carbonyl group. A more dramatic effect is seen if the exocyclic N-4 carbonyl group is removed entirely; a 200-fold in drop in potency is observed for compound **20f** (IC_{50} = 0.23 μM), underscoring the importance of the carbonyl group in compound **20d** to overall inhibition. Compound **20h**, the most potent compound in our studies, shows <1 nM inhibition against TrkA (IC_{50} = 0.0006 μM), superior to its steric isostere **20e** (IC_{50} = 0.021 μM). Finally, a chiral center adjacent to the carbonyl group does not affect TrkA inhibition; the enantiomeric pair **20i** (IC_{50} = 0.001 μM) and **20j** (IC_{50} = 0.001 μM) shows the same level of inhibition.

To better understand the SAR of these inhibitors, a binding model of **20i** in a homology model of the kinase domain of TrkA was generated. The TrkA homology model was built using the crystal structure of Muscle-specific kinase (MuSK)[15] as a template with the structure prediction algorithm implemented in the software Prime.[16] Compound **20i** was manually docked in the ATP binding site of the model (see Fig. 2) using the small molecule X-ray structure geometry of an analog of **20i** (data not shown), and the crystal structures of kinase complexes of related chemotypes as guidance. A pair of hydrogen bond interactions is proposed between the nitrogen of the thiazole ring and the backbone NH of Met592 (part of the hinge region) and between the anilino NH and the carbonyl oxygen of Met592; similar

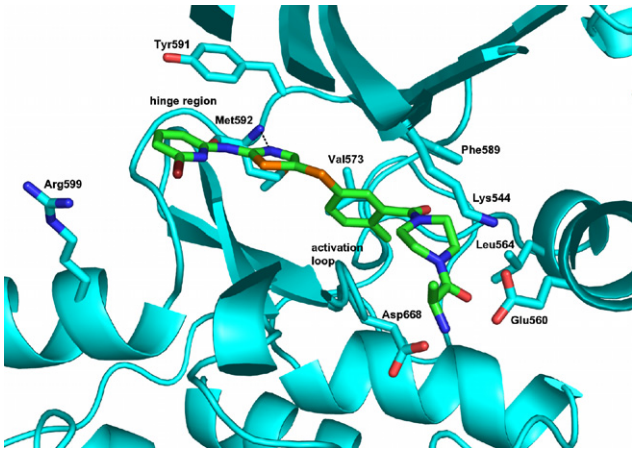

Figure 2. Binding model of **20i** in the ATP binding site of a homology model of TrkA. Carbon atoms of **20i** are in green. Carbon atoms of protein are in cyan. Hydrogen bonds are indicated by block dotted lines. Image created with Pymol from DeLano Scientific LLC, San Carlos, CA, USA. http://www.pymol.org.

interactions are also observed with another aminothiazole kinase inhibitor.[17] The pyridine ring points toward the surface-exposed portion of the hinge region. The thioaryl group probes a mostly hydrophobic pocket which includes the gatekeeper residue Phe589 and Leu564 of helix-αC. The choice of using MuSK tyrosine kinase as the template was reinforced by the high sequence homology with TrkA and by the observation that the kinase was in an inactive conformation; i.e., the activation loop folds back toward the ATP binding site creating a larger pocket near the gatekeeper than is normally found with an active conformation. The inactive conformation allows the substituted thioaryl group to occupy the buried specificity region vacated by the portion of the activation loop following Asp668 of the DFG motif. This model is consistent with some key SAR observations. With respect to the terminal pyridine ring, both compounds **11d** (C-6 substituent is hydrogen) and **11g** (C-6 substituent is methyl) are 5- to 10-fold less active than compound **11e** (C-6 substituent is bromine). The model suggests that the hydrogen is too small, and the methyl group not polarized to maximize polar and van der Waals interactions with the surface-exposed specificity pocket which includes residues Tyr591 and Arg599. The difference in activity of the methyl-substituted thioaryl ring analog **11c** and the un-substituted **11e** may due to the methyl filling in a small pocket near Val573. The ortho-methyl may also reduce the conformational space toward available space. The size of the buried specificity pocket is limited as evidenced by the loss of activity of the larger ring of **20a** versus **11h**. However, one cannot rule out that the seven-membered ring may also direct the terminal N-4 carbonyl toward unfavorable protein contacts. A dramatic loss of activity (>200-fold loss) is observed when the carbonyl group is removed (compound **20f**) from the control compound **20d**. While it is not clear whether this is the consequence of simple hybridization, the removal of the carbonyl group may remove a potential interaction with the conserved Lys544. In addition, the terminal amino group has the opportunity to hydrogen bond with the conserved Asp668 and/or Glu560.

As shown in Table 5, a select set of TrkA inhibitors were evaluated in cell based proliferation assay.[18] CD8-TrkA is rat kidney epithelium cells (RKE) with constitutively activated TrkA; V3.1 is its control TrkA-null cell line whose proliferation is not dependent on TrkA signaling pathway. SH-SY5Y is a human neuroblastoma cell-line that expresses TrkA. Inactive TrkA inhibitor **11k** ($IC_{50} > 5\ \mu M$) shows essentially no anti-proliferative effect in both CD8-Trk A and SH-SY5Y cells ($IC_{50} > 10\ \mu M$). In contrast, potent inhibitors of TrkA (**20j**, **11c**, **11v**, **11t**, **11w**, **20h**, and **20i**) show consistent anti-proliferative effects ($IC_{50} < 0.5\ \mu M$) in CD8-TrkA cells with a ~10-fold window against the vector V3.1. In the SH-SH-5Y cells, the level of anti-proliferation is 2- to 8-fold less than that observed for the CD8-TrkA cells. Further evidence that proliferation is linked to TrkA inhibition comes from the measurement of phospho-TrkA levels. In CD8-TrkA cells, the level of phospho-TrkA and phospho-ERK1 and 2 (a downstream kinase) is down-regulated with increasing concentration of inhibitor **11t** (data not shown), consistent with the mechanism of inhibition, and supports the observation that proliferation is likely due to TrkA inhibition.

Compounds evaluated in proliferation assay were also tested against a limited set of kinases, as shown in Table 6. All compounds show good selectivity: a 6- to 500-fold window against CDK2, as well as against Met, IGF1R, and VEGFR, consistent with the observation that anti-proliferative effects are driven by TrkA inhibition.

In summary, we have identified 2-amino-5-(thioaryl)thiazoles as potent inhibitors of TrkA ($IC_{50} < 1$ nM) and provided structural basis for the key SAR observations. The intrinsic biochemical potency against TrkA and corresponding anti-proliferative effects and biochemical markers, together with the kinase selectivity, are suggestive that TrkA inhibition is responsible for their cellular response. The

Table 6. Kinase selectivity of TrkA inhibitors

Compound	Trk A IC_{50} (μM)	CDK2 IC_{50} (μM)	IGF1R IC_{50} (μM)	Met IC_{50} (μM)	VEGFR IC_{50} (μM)
11c	0.001	0.49	>1.0	>1.0	>25
11w	0.03	0.18	>1.0	>1.0	8%[b]
20h	0.0006	0.54	>1	0.43	NT
20i	0.001	0.52	0.36	>1.0	NT
20j	0.001	0.23	0.7	0.17	NT

[b] % inhibition at 2 μM.

evaluation of these compounds in in vivo models will be reported in due course.

References and notes

1. Nakagawara, A. *Cancer Lett.* **2001**, *169*, 107.
2. Huang, E. J.; Reichardt, L. F. *Annu. Rev. Biochem.* **2003**, *72*, 609.
3. Schramm, A.; Shulte, J. H.; Astrahantseff, K.; Apostolov, O.; Limpt, V.; Sieverts, H.; Kuhfittig-Kulle, S.; Pfeiffer, P.; Versteeg, R.; Eggert, A. *Cancer Lett.* **2005**, *228*, 143.
4. Florenes, V. A.; Malanddsmo, G. M.; Holm, R.; Reich, R.; Lazarovici, P.; Davidson, B. *Am. J. Clin. Pathol.* **2004**, *122*, 412.
5. Davidson, B.; Reich, R.; Lazarovici, P.; Nesland, J. M.; Skered, M.; Risberg, B.; Trope, C. G.; Florenes, V. A. *Clin. Cancer Res.* **2003**, *9*, 2248.
6. Zhang, Y.; Dang, C.; Ma, Q.; Shimahara, Y. *Oncol. Reports* **2005**, *14*, 161.
7. Ruggeri, B. A.; Miknyoczki, S. J.; Singh, J.; Hudkins, R. L. *Curr. Med. Chem.* **1999**, *6*, 845.
8. George, D. J.; Dionne, C. A.; Jani, J.; Angeles, T.; Murakata, C.; Lamb, J.; Issacs, J. T. *Cancer Res.* **1999**, *59*, 2395.
9. Undevia, S. D.; Vogelzang, N. J.; Mauer, A. M.; Janisch, L.; Mani, S.; Ratain, M. J. *Invest. New Drugs* **2004**, *22*, 449.
10. Wood, E. R.; Kuyper, L.; Petrov, K. G.; Hunter, R. N., III; Harris, P. A.; Lackey, K. *Biorg. Med. Chem. Lett* **2004**, *14*, 953.
11. Lippa, B.; Morris, J.; Corbett, M.; Kwan, T. A.; Noe, M. C.; Snow, S. L.; Gant, T. G.; Mangiaracina, M.; Coffey, H. A.; Foster, B.; Knauth, E. A.; Wessel, M. D. *Biorg. Med. Chem. Lett.* **2006**, *16*, 3444.
12. Das, J.; Liu, C.; Moquin, R.; Lin, J.; Furch, J. A.; Spergel, S. H.; McIntyre, K. W.; Shuster, D. J.; O'Day, K. D.; Penhallow, B.; Hung, C.-H.; Kanner, S. B.; Lin, T.-A.; Dodd, J. H.; Barrish, J. C.; Wityak, J. *Biog. Med. Chem. Lett.* **2006**, *16*, 2411.
13. Das, J.; Furch, J. A.; Liu, C.; Moquin, R.; Lin, J.; Spergel, S. H.; McIntyre, K. W.; Shuster, D. J.; O'Day, K. D.; Penhallow, B.; Hung, C.-H.; Doweyko, A. M.; Kamath, A.; Zhang, H.; Marathe, P.; Kanner, S. B.; Lin, T.-A.; Dodd, J. H.; Barrish, J. C.; Wityak, J. *Biog. Med. Chem. Lett.* **2006**, *16*, 3706.
14. Values are means of three experiments with standard deviation of less than 15%. Assay conditions: ATP concentration at 10 μM, reaction time = 35 min, enzyme concentration (μg/well) = 0.008, Substrate concentration (μg/well) = 0.625 at 30 °C.
15. Till, J. H.; Becerra, M.; Watty, A.; Lu, Y.; Ma, Y.; Neubert, T. A.; Burden, S. J.; Hubbard, S. R. *Structure* **2002**, *10*, 1187.
16. Schrodinger, L. L. C. 32nd Floor, Tower 45, 120 West Forty-Fifth Street, New York, 10036, 2003.
17. Tokarski, J. S.; Newitt, J. A.; Chang, C. Y. J.; Cheng, J. D.; Wittekind, M.; Kiefer, S. E.; Kish, K.; Lee, F. Y. F.; Borzilleri, R.; Lombardo, L. J.; Xie, D.; Zhang, Y.; Klei, H. E. *Cancer Res.* **2006**, *66*, 5790.
18. RK3E vector (pcDNA3.1, V3.1) or CD8-TrkA transfectants and SH-SY-5Y cells were cultured in DMEM + 10% FBS or RPMI1640 + 10% FBS, respectively. Confluency after 3 days: 80% for CD8-TrkA and V3.1cell lines; 65% for SH-SY5Y. All cells were plated in media containing 2.5% FBS (SH-SY-5Y) or 10% FBS (RK3E transfectants) and compounds administered the next day. After 3 days treatment, the cells were pulsed with 10 μl of diluted $\{^3H\}$-thymidine at 4 μCi/ml for 3 h. Values are means of three experiments.